

# Interaction of G Protein $\beta$ Subunit with Inward Rectifier $K^+$ Channel Kir3

QI ZHAO, TAKEHARU KAWANO, HIROKO NAKATA, YASUKO NAKAJIMA, SHIGEHIRO NAKAJIMA, and TOHRU KOZASA

*Departments of Pharmacology (Q.Z., H.N., S.N., T.Ko.) and Anatomy and Cell Biology, College of Medicine, University of Illinois at Chicago, Illinois 60612 (T.Ka., Y.N.)*

Received May 12, 2003; accepted August 8, 2003

This article is available online at <http://molpharm.aspetjournals.org>

## ABSTRACT

G protein  $\beta\gamma$  subunits bind and activate G protein-coupled inward rectifier  $K^+$  (GIRK) channels. This protein-protein interaction is crucial for slow hyperpolarizations of cardiac myocytes and neurons. The crystal structure of  $G\beta$  shows a seven-bladed propeller with four  $\beta$  strands in each blade. The  $G\beta/G\alpha$  interacting surface contains sites for activating GIRK channels. Furthermore, our recent investigation using chimeras between  $G\beta_1$  and yeast  $\beta$  (STE4) suggested that the outer strands of blades 1 and 2 of  $G\beta_1$  could be an interaction area between  $G\beta_1$  and GIRK. In this study, we made point mutations on suspected residues on these outer strands and investigated their ability to activate GIRK1/GIRK2 channels. Mutations at Thr-86, Thr-87, and Gly-131, all located on the loops between  $\beta$ -strands, substantially reduced GIRK channel activation, sug-

gesting that these residues are  $G\beta$ /GIRK interaction sites. These mutations did not affect the expression of  $G\beta_1$  or its ability to stimulate PLC $\beta_2$ . These residues are surface-accessible and located outside  $G\beta/G\alpha$  interaction sites. These results suggest that the residues on the outer surface of blades 1 and 2 are involved in the interaction of  $G\beta\gamma$  with GIRK channels. Our study suggests a mechanism by which different effectors use different blades to achieve divergence of signaling. We also observed that substitution of alanine for Trp-332 of  $G\beta_1$  impaired the functional interaction of  $G\beta_1$  with GIRK, in agreement with the data on native neuronal GIRK channels. Trp-332 plays a critical role in the interaction of  $G\beta_1$  with  $G\alpha$  as well as all effectors so far tested.

The family of G protein-coupled inward rectifier  $K^+$  channels (GIRK; Kir3) plays important roles in physiological functions; the activity of the GIRK channels is a major determinant of excitability in many kinds of cells, including cardiac myocytes and neurons (Sakmann et al., 1983; Dascal et al., 1993; Kubo et al., 1993; Wickman and Clapham, 1995; Stanfield et al., 2002). The activity of GIRK channels, in turn, is regulated by G proteins (Breitwieser and Szabo, 1985; Pfaffinger et al., 1985; Kurachi et al., 1986). Furthermore, the  $\beta\gamma$  subunits ( $G\beta\gamma$ ) but not the  $\alpha$  subunit ( $G\alpha$ ) of G proteins were shown to activate the GIRK channels (Logothetis et al., 1987; Ito et al., 1992; Reuveny et al., 1994; Huang et al., 1995; Krapivinsky et al., 1995). Thus, the interaction between  $G\beta\gamma$  and GIRK is a crucial process for the physiological functions of the brain and the heart and, as such, is likely to be one of the sites for pharmacological interventions. Despite its importance, the molecular mechanism of this protein-protein interaction is poorly understood. One approach to clarify this interaction is to investigate the events

that take place on the side of the  $K^+$  channel. Another is to elucidate the processes occurring on the  $G\beta\gamma$  molecules.

The aim of this study was to further clarify the residues of the  $G\beta$  molecule that interact with GIRK. X-ray crystallography has revealed that  $G\beta$  is a seven-bladed propeller structure with four antiparallel  $\beta$  strands for each blade.  $G\alpha$  interacts with  $G\beta$  through the top surface of the propeller. The outer  $\beta$ -strands of each blade form the outer surface of the torus-like structure (Wall et al., 1995; Lambright et al., 1996; Sondek et al., 1996). Because  $G\beta$  is capable of interacting with downstream effectors only if  $G\alpha$  is detached from  $G\beta$ , it has been assumed that the interaction sites of  $G\beta$  with  $G\alpha$  may also be the sites that interact with various effectors. Indeed, mutagenesis studies have identified various  $G\alpha$ -contacting residues of  $G\beta$  that are crucial for the interaction between  $G\beta\gamma$  and various effectors, such as phospholipase C $\beta$ s (PLC $\beta$ s), adenylyl cyclases, and GIRK channels (Ford et al., 1998; Li et al., 1998).

The  $G\alpha$ -interacting surface of  $G\beta$  may not be the only region to bind the effectors. Albsoul-Younes et al. (2001) constructed a set of  $G\beta_1$  chimera proteins by replacing a sequence on or near the outermost strand of each of the blades with the corresponding sequence in yeast  $G\beta$  (STE4).

This work was supported by National Institutes of Health grants MH57837 (to S.N.), AG06093 (to Y.N.), GM61454, and NS/GM41441, and by American Heart Association Grant (to T.K.). T.K. is an established investigator of American Heart Association.

**ABBREVIATIONS:** GIRK, G protein-coupled inward rectifier  $K^+$  channels; PLC, phospholipase C; HEK, human embryonic kidney; DMEM, Dulbecco's modified Eagle's medium.

These proteins were tested for their ability to activate native GIRKs in brain neurons. The results indicated that the chimeras on the outer segments of blades 1 and 2 (called D1 and CD2) significantly impaired the GIRK activation (Albsoul-Younes et al., 2001), suggesting that these locations are important for the interaction between G $\beta$  and GIRKs. These locations do not belong to the interaction sites between G $\beta$  and G $\alpha$ .

Because we know that the outer segments of blades 1 and 2 are crucial for the G $\beta$ /GIRK interaction, the next step is to precisely identify the amino acid residues in these regions that are crucial for the GIRK activation. In the present experiments, we introduced point mutations on each of the nonconserved (between G $\beta$ 1 and STE4) residues on D1 and CD2 to its corresponding residue in STE4 (Albsoul-Younes et al., 2001). Each of these mutant G $\beta$ 1 cDNAs was expressed in human embryonic kidney (HEK) 293 cells and was tested for the ability to produce inwardly rectifying K<sup>+</sup> currents. In this way, we have identified three G $\beta$ 1 residues located on the outer strands of blade1 and blade 2; mutations of these residues impaired the GIRK activation and therefore may play a crucial role in GIRK activation. The results suggest that in addition to the G $\alpha$ -interacting surface, these residues on the outer surface of blades 1 and 2 are specifically involved in the interaction of G $\beta$  with GIRK channels. Recently, Mirshahi et al. (2002) also identified 2 residues on blades 1 and 2 that could be the interaction sites with GIRK but not with G $\alpha$ . Altogether, therefore, 5 residues are putative sites at which G $\beta$ /GIRK interaction would take place outside the G $\beta$ /G $\alpha$  interface. An abstract of the present work has appeared (Zhao et al., 2002).

## Materials and Methods

**Molecular Biology.** GIRK1 and GIRK2 cDNAs were from the rat. G $\beta$ 1 cDNA was from the mouse and G $\gamma$ 2 cDNAs was from the bovine. All cDNAs used were subcloned into pCMV5 vector (Anderson et al., 1989). Point mutations were introduced by using the QuikChange site-directed mutagenesis kit (Stratagene; La Jolla, CA). The mutations were verified by the sequence facility at the University of Chicago.

**Cell Culture and Transfection.** HEK293 cells were maintained in Dulbecco's modified Eagle's medium (DMEM) with 10% fetal bovine serum (Invitrogen, Carlsbad, CA) at 37°C with 10% CO<sub>2</sub>. Transient transfections of HEK293 cells were performed with Effectene (QIAGEN, Valencia, CA) according to the manufacturer's protocol. The total amount of cDNAs for the same experiment was kept constant by adding empty vectors.

**Electrophysiology.** HEK293 cells in 60-mm dishes were transfected with cDNAs of wild-type or mutant G $\beta$ 1, G $\gamma$ 2, GIRK1, GIRK2, and GFP. The amount of each cDNA was 0.3  $\mu$ g, except 0.1  $\mu$ g for GFP. Twenty-four hours later, the cells were replated onto 35-mm dishes. The dish has a small well (about 1.2 cm in diameter) that was coated with rat-tail collagen (Roche Molecular Biochemicals, Indianapolis, IN). Forty-eight to 56 h after transfection, the whole-cell patch clamp was performed on the stage of a fluorescence inverted microscope. We did experiments on isolated cells with GFP fluorescence. The bathing solution contained 146 mM sodium gluconate, 10 mM potassium gluconate, 2.4 mM CaCl<sub>2</sub>, 1.3 mM MgCl<sub>2</sub>, 5 mM HEPES-NaOH, and 0.5  $\mu$ M tetrodotoxin, pH 7.4. The pipette solution contained 151 mM K gluconate, 5 mM HEPES-KOH, 0.5 mM EGTA-KOH, 0.1 mM CaCl<sub>2</sub>, 4 mM MgCl<sub>2</sub>, 3 mM Na<sub>2</sub>-ATP, and 0.2 mM GDP, pH 7.2. Membrane potentials were corrected for the liquid junction potential between the pipette solution and the bathing solution (the bathing solution side was 7 mV positive). Cell capaci-

tance was determined by cancellation of the transient responses to square-wave voltage inputs as directed in the user's manual for the EPC-7 patch clamp (List Electronic, Darmstadt, Germany). Series resistance was compensated electronically, usually by about 60%, and the remaining resistance was compensated mathematically by a linear approximation. The pCLAMP programs (version 6.03; Axon Instruments, Inc.) were used for the acquisition and analysis of the data. Recordings were performed at room temperature. Statistical results were expressed as mean  $\pm$  S.E.M.

**Western Blot Analysis.** HEK293 cells in 35-mm dishes were transfected with 0.75  $\mu$ g of G $\beta$ 1 and 0.75  $\mu$ g of FLAG-G $\gamma$ 2. Forty-eight h after transfection, the cells were harvested and lysed on ice for 20 min in 200  $\mu$ l of lysis buffer (20 mM HEPES-NaOH at pH 7.5, 150 mM NaCl, 5 mM MgCl<sub>2</sub>, 1 mM EDTA, 1 mM EGTA, 10 mM NaF, 25 mM  $\beta$ -glycerophosphate, 1 mM Na<sub>3</sub>VO<sub>4</sub>, 2  $\mu$ g/ml aprotinin, 10  $\mu$ g/ml leupeptin, 10  $\mu$ g/ml pepstatin A, 0.5% Triton X-100, and 10% glycerol). Lysates were centrifuged at 15,000g for 20 min at 4°C. The supernatants were heated at 100°C for 5 min in a sample buffer (50 mM Tris-HCl, pH 6.8, 8% glycerol, 1% SDS, 2% 2-mercaptoethanol, and 0.008% bromophenol blue). Aliquots (20  $\mu$ l) of the samples were loaded on 5% stacking, 15% separating SDS-PAGE gel. After electrophoresis, the proteins were transferred to a BA81 nitrocellulose membrane and blocked with blocking buffer (50 mM Tris-HCl, pH 8.0, 2 mM CaCl<sub>2</sub>, 80 mM NaCl, 5% skim milk, 0.2% Nonidet P-40, and 0.02% NaN<sub>3</sub>). The proteins were detected by G $\beta$  (T-20) polyclonal antibody (Santa Cruz Biotechnology, Santa Cruz, CA) and anti-FLAG M2 monoclonal antibody (Sigma, Saint Louis, MO). The bound antibodies were visualized by an enhanced chemiluminescence detection system, using horseradish peroxidase-conjugated anti-rabbit or anti-mouse Ig secondary antibodies (Amersham Bioscience, Arlington Heights, IL).

**PLC $\beta$  Assay in HEK293 Cells.** HEK293 cells at 60 to 70% confluence in 24-well plates were transfected with PLC $\beta$ 2, G $\beta$ 1 (wild type or mutant), G $\gamma$ 2, and G $\alpha$ <sub>o</sub>. The total amount of cDNA was 0.8  $\mu$ g per well. One day after transfection, the cells were labeled with 2  $\mu$ Ci/ml [<sup>3</sup>H]inositol in 0.5 ml of inositol-free DMEM with 1% fetal bovine serum for 24 h. The next day, the cells were washed for 10 min and then stimulated for 50 min at 37°C with 0.5 ml of inositol-free DMEM supplemented with 25 mM HEPES, pH 7.4, and 10 mM LiCl. The reactions were terminated by 20 mM formic acid (0.75 ml), and the cells were incubated at 4°C for 30 min. The samples were neutralized to pH 7 to 8 by 100  $\mu$ l of 3% ammonium hydroxide, collected, and centrifuged at 15,000 rpm for 5 min. The supernatants were loaded on 1 ml of Dowex AG 1-X8 columns pre-equilibrated with 10 ml of 4 M ammonium formate and 0.2 M formic acid followed by 5 ml of 0.18% ammonium hydroxide solutions. The flow-through of the sample and of the 1 ml of 0.18% ammonium hydroxide solution loaded after the sample was collected as the inositol fraction. The columns were washed with 4 ml of 40 mM ammonium formate and 0.1 M formic acid. The inositol phosphates were eluted with 1 ml of 4 M ammonium formate and 0.2 M formic acid. The inositol fraction and the inositol phosphate fraction were measured by liquid scintillation counting.

## Results

**Activation of GIRK Currents by G $\beta$ 1 $\gamma$ 2 Cotransfection in HEK293 Cells.** We used HEK293 cells as a heterologous expression system to test the ability of wild-type and mutant G $\beta$ s to activate GIRK channels. GIRK1/GIRK2 channel subunits alone or GIRK1/GIRK2 together with G $\beta$ 1 $\gamma$ 2 were expressed. Whole-cell currents were evoked by a series of voltage steps from -127 to -27 mV at a 10-mV increment. Holding potential was -77 mV. Figure 1, A and B, shows that cells transfected with GIRK1/GIRK2 and G $\beta$ 1 $\gamma$ 2 cDNAs produced large currents. The currents showed inward rectification and the reversal potential ( $-65.4 \pm 0.8$  mV;  $n = 28$ )

corresponded to the K<sup>+</sup> equilibrium potential ( $E_K$ ) (−68.4 mV).

The current amplitudes at −97 mV were chosen to represent the capability of various G $\beta_1$  subunits to activate the GIRK current (Fig. 1C). Transfection with wild-type G $\beta_1\gamma_2$  plus GIRK1/GIRK2 evoked large currents, whereas cells transfected with GIRK1/GIRK2 (without G $\beta_1\gamma_2$ ) produced smaller currents. These small currents would have been derived from the transfected GIRK1/GIRK2 activated by the endogenous G $\beta\gamma$ . If neither GIRK1/GIRK2 nor G $\beta\gamma$  was transfected, the current was very small (about one third of the current with GIRK1/GIRK2 only) (Kawano et al., 1999).

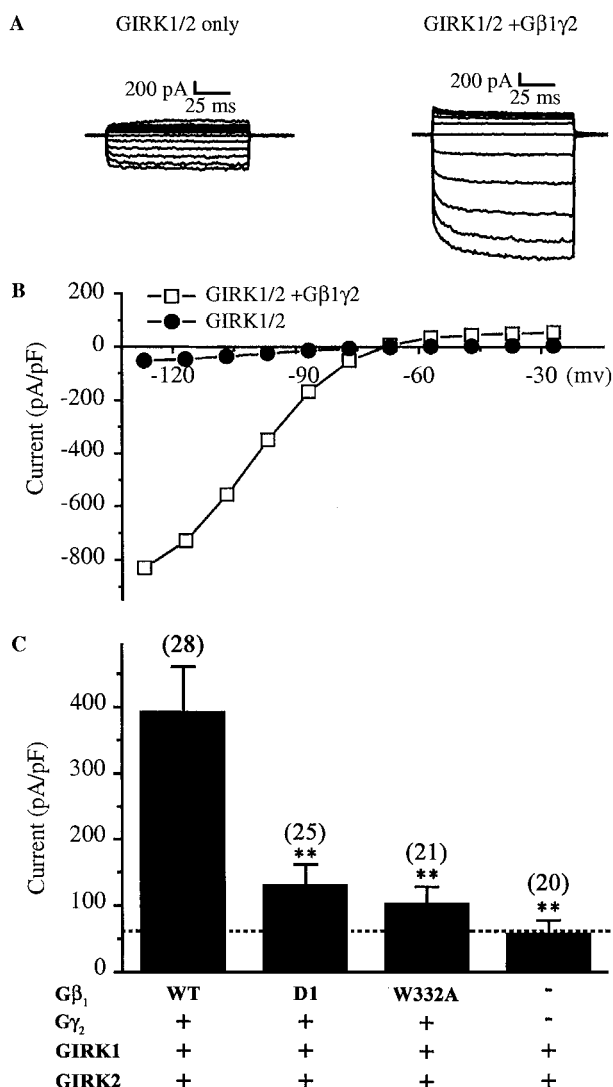


**Fig. 1.** Activation of GIRK channels by G $\beta_1\gamma_2$  in HEK293 cells. Cells were transfected with wild-type or mutant G $\beta_1$  together with G $\gamma_2$ , GIRK1, and GIRK2. Whole-cell currents were evoked by voltage steps from −127 to −27 mV at a 10-mV increment. Holding potential was −77 mV. A, samples of current traces recorded from cells transfected with GIRK1/GIRK2, either with or without G $\beta_1\gamma_2$ . B, the current-voltage relation derived from the current traces shown in A. Currents were expressed in reference to the cell capacitance. □, current from a cell transfected with GIRK1/GIRK2 together with G $\beta_1\gamma_2$ ; ●, current from a cell transfected with GIRK1/GIRK2 only. C, G $\beta_1$  mutants D1 and W332A are less effective in activating the GIRK channel. Whole-cell currents at −97 mV were used for statistics. \*\*,  $p < 0.01$  (analysis of variance and Bonferroni post tests). The dashed line indicates the current level produced by endogenous  $\beta\gamma$ .

This small current would have originated from unknown channels endogenous in HEK293 cells (Kawano et al., 1999).

In addition, Fig. 1C shows GIRK1/GIRK2 currents induced by two G $\beta_1$  mutants, the chimera D1 and a point mutation W332A. The D1 mutant, the same as used by Albsoul-Younes et al. (2001), was generated by replacing the G $\beta_1$  sequence on and near the outer strand of blade 1 (S84 to P94) with the corresponding yeast  $\beta$  (STE4) sequences (Fig. 2). W332A is a point mutant on the G $\alpha$ -contacting surface of G $\beta_1$  (Albsoul-Younes et al., 2001). Both the chimera and W332A produced substantially smaller GIRK current than the wild-type G $\beta_1\gamma_2$ . These data on the genetically identified GIRK1/GIRK2 channels coincide well with the previous data on native GIRK channels in locus ceruleus neurons (Albsoul-Younes et al., 2001).

**Identifying the Critical Residues in the D1 Region for G $\beta$ -GIRK Interaction.** We mutated each nonconservative G $\beta_1$  residue over the D1 mutation region (i.e., from Ser84 to Pro94) to its corresponding STE4 residue (Fig. 2A);

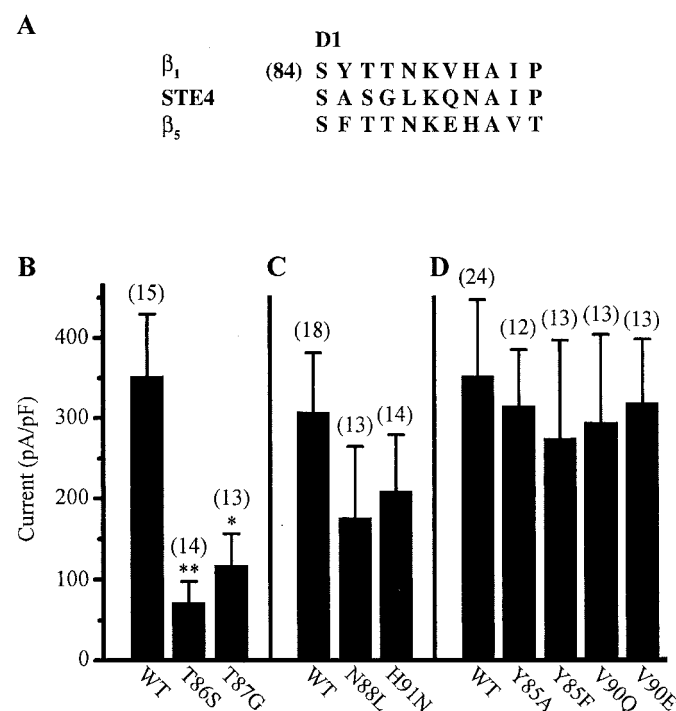


**Fig. 2.** A, sequence alignment of G $\beta_1$ , yeast G $\beta$  (STE4), and G $\beta_5$  in the D1 regions. B to D, effects of single amino acid mutations in the D1 region on the activation of GIRK channels. The mutants were made by replacing a wild-type G $\beta_1$  residue with the corresponding yeast G $\beta$  residue, except for Y85F and V90E, in which the mutants were made by replacing the G $\beta_1$  residue with the corresponding G $\beta_5$  residue. Before the start of the experiments, we had planned to divide these eight mutants into three groups (see below for the categorization), and for each group we compared the mutants with wild type. B, in this group, T86S and T87G were compared with wild-type G $\beta_1$ . These two mutants comprise the first two, in which the STE4 residue is different from the corresponding residue of wild-type G $\beta_1$ , yet the G $\beta_5$  residue is the same as in G $\beta_1$ . T86S and T87G showed less ability to stimulate GIRK currents than the wild type. \*,  $p < 0.05$ ; \*\*,  $p < 0.01$ , respectively (analysis of variance and Bonferroni post tests). C, the G $\beta_1$  mutants, N88L and H91N, are the next two mutants, in which the STE 4 residue is different from the corresponding wild-type G $\beta_1$  residue, yet the G $\beta_5$  residue is the same as in G $\beta_1$ . These mutants produced GIRK current not significantly different from that of the wild-type G $\beta_1$ . D, in these G $\beta_1$  mutants, Y85A, Y85F, V90Q, and V90E, the corresponding residues for STE4 as well as for G $\beta_5$  are different from those of G $\beta_1$ . All these mutants produced GIRK current activation not significantly different from that of wild-type G $\beta_1$ .



these are Y85A, T86S, T87G, N88L, V90Q, and H91N. We noticed that two residues, Tyr85 and Val90, are nonconservative not only between  $\beta 1$  and STE4 but also between  $\beta 1$  and  $\beta 5$ . The subunit G $\beta 5$  is a distinct member of the G $\beta$  family. Instead of activating GIRK channels, G $\beta 5$  inhibits GIRK currents (Lei et al., 2000). We therefore made two additional mutants, Y85F and V90E, by replacing the G $\beta 1$  residue with the corresponding residue of G $\beta 5$ .

Each of these mutant G $\beta 1$  cDNAs was cotransfected with GIRK1/GIRK2 and G $\gamma 2$ . Figure 2, B, C, and D, summarizes the GIRK current stimulation by these G $\beta 1$  mutants in D1 region. Compared with wild-type G $\beta 1\gamma 2$ , mutants T86S and T87G were much less effective in activating GIRK currents ( $p < 0.01$  and  $p < 0.05$ , respectively) (Fig. 2B). No other mutants showed any significant differences from the wild-type  $\beta 1$  in their ability to enhance the GIRK current (Fig. 2, C and D).

**Identifying the Critical Residues in the CD2 Region for G $\beta$ -GIRK Interaction.** The result obtained by Albsoul-Younes et al. (2001) indicates that the G $\beta 1$  mutant CD2 is less capable of activating GIRK channels in locus ceruleus neurons. In the CD2 mutant, the G $\beta 1$  sequence (Leu126-Asn132) on the loop connecting the two outer strands of blade 2 was replaced with its counterpart in STE4 (Fig. 3A). We generated five G $\beta 1$  mutants, L126V, T128S, R129K, G131V, and N132A, by mutating each of the nonconservative G $\beta 1$  residues over the CD2 region to its corresponding STE4 residue. We also made one deletion mutation, K127 $\Delta$  (Fig. 3A). These mutants were tested for their ability to stimulate GIRK channels coexpressed in HEK293 cells. As shown in Fig. 3B, G $\beta 1$  mutant G131V showed a substantially lower ability to activate the GIRK current compared with wild type. All other mutants in the CD2 region were able to enhance GIRK current in a manner not significantly different from that of the wild type (Fig. 3, B and C).

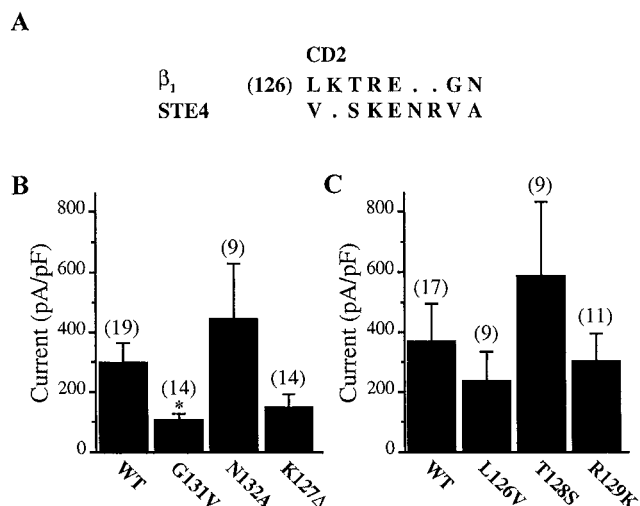


**Fig. 3.** A, sequence alignment of G $\beta 1$  and yeast G $\beta$  (STE4) in the CD2 region. B and C, effects of single amino acid mutations in the CD2 region on GIRK activation. Each nonconservative G $\beta 1$  residue was mutated to its counterpart in STE4. Before the start of the experiments, we had planned to divide the mutants into 2 groups; for each group, we measured both the response to the wild type and to the mutants. B, G131V produced a much smaller GIRK current ( $p < 0.05$ ), whereas N132A and K127 $\Delta$  produced currents that were not significantly different from wild-type G $\beta 1$ . C, mutants L126V, T128S, and R129K produced currents not significantly different from wild-type G $\beta 1$ .

**Basal Currents or Agonist-Induced Currents.** Mirshahi et al. (2002), by using the oocyte heterologous system, identified two G $\beta$  residues, Ser67 and Thr128. Both of these residues are located outside the G $\beta$ /G $\alpha$  contact region and are likely to be interaction sites between G $\beta$  and GIRK channels. They observed that mutations of these residues inhibited the GIRK “basal currents”, which are presumably activated by the endogenous G $\beta\gamma$ . One might ask whether our mutants impair the generation of the GIRK basal current.

In HEK293 cells, unlike the oocyte system, the “basal GIRK current” is relatively small compared with the current induced by exogenous G $\beta 1\gamma 2$  (compare the first column with the fourth column in Fig. 1C). This makes it difficult to determine whether our mutations (T86S, T87G, and G131V) impaired the “basal GIRK current”. From our results, therefore, we can conclude only that our mutants impaired the GIRK current stimulated by exogenous G $\beta 1\gamma 2$ .

**Expression of G $\beta 1$  Mutants in HEK293 Cells.** To examine the expression levels of the G $\beta 1$  mutants, HEK293 cells expressing G $\beta 1$  and FLAG-G $\gamma 2$  were subjected to the Western blot analysis. An antibody raised against a peptide at the carboxyl terminus of G $\beta 1$  (T-20, Santa Cruz Biotechnology) was used for immunoblotting. Figure 4 shows representative Western blots from cells expressing the G $\beta 1$  mutants. Low levels of G $\beta$  (endogenous G $\beta$ ) (the leftmost lane) could be detected in cells transfected with vectors alone (Fig. 4, A and B). All three mutant G $\beta 1$ s that had a low ability to activate GIRK channels—T86S, T87G, and G131V—were expressed at a level comparable with that of the wild-type G $\beta 1$  (Fig. 4A); thus, the functional impairment is not caused by the differences in the expression level. All other G $\beta 1$  mutants that can activate the channels as effectively as wild type were also expressed at a level similar to that of the wild-type  $\beta 1$  (Fig. 4B).

It is noted that expression of G $\gamma 2$  in the Western blot is fairly variable in the example of Fig. 4. However, inspection

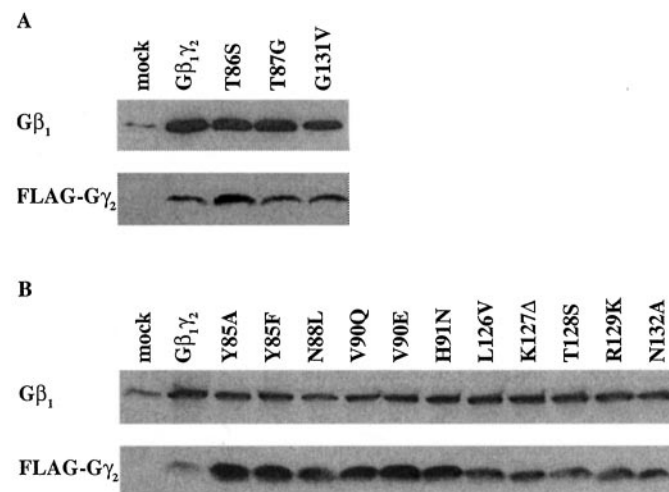


**Fig. 4.** Point mutations did not affect the expression level of G $\beta 1$  in HEK293 cells. Cells were transfected with G $\beta 1$  and FLAG-G $\gamma 2$ . The first lanes (mock) show blots from cells transfected with empty vectors. A small amount of endogenous G $\beta$  was detected in these cells. A, despite their reduced effectiveness in activating channels, mutants T86S, T87G, and G131V were expressed at a level comparable with that of the wild-type G $\beta 1$ . B, all other G $\beta 1$  mutants in the D1 and CD2 regions, which did not significantly differ from wild type in current stimulation, were expressed as efficiently as wild type.

of all Western blots obtained in this experiment (five runs for Fig. 4A and six runs for Fig. 4B) indicated that there seemed to be no correlation between the Western blot expression of G $\gamma$ 2 and the functional ability of various mutants and the wild type. It is thus unlikely that the functional defect of the mutants is caused by differences in the G $\gamma$ 2 expression.

**Activation of PLC $\beta$ 2 by G $\beta$ 1 Mutants.** G $\beta\gamma$  regulates not only GIRKs but also several other effectors including PLC $\beta$ s. To test whether the G $\beta$ 1 mutants retain their ability to activate PLC $\beta$ , we transfected HEK293 cells with PLC $\beta$ 2, G $\beta$ 1, and G $\gamma$ 2 in either the absence or the presence of G $\alpha_o$ . For each sample, the amount of inositol phosphates produced by the lithium treatment was normalized to the total amount of free inositol and inositol phosphates. As shown in Fig. 5, transfection of PLC $\beta$ 2 alone resulted in the production of a small amount of inositol phosphates. The wild-type G $\beta$ 1 $\gamma$ 2 caused a 7-fold increase in inositol phosphate production, which could be completely suppressed to the basal level by cotransfection of G $\alpha_o$ . The bottom panel shows immunoblots of the samples from the same experiment. Without G $\beta$ 1 $\gamma$ 2 sequestration by G $\alpha_o$ , the expression level of G $\beta$ 1 was more or less proportional to the amount of inositol phosphate produced. Taken together, the elevation of the inositol phosphate production represented the activation of PLC $\beta$ 2 by G $\beta$ 1 $\gamma$ 2 coexpressed in the cells. In conclusion, this experiment shows that despite their inefficiency at activating the K $^+$  channels, the G $\beta$ 1 mutants T86S, T87G, and G131V were as effective as wild type in stimulating PLC $\beta$ 2 activity. In addition, the inhibitory effect of coexpression of G $\alpha_o$  on PLC $\beta$ 2 activation by these mutants suggests that they can interact with G $\alpha_o$  in a way similar to wild-type G $\beta$ 1.

Albsoul-Younes et al. (2001) observed that the CD2 mutant, in which the G $\beta$ 1 segment near the outer strand of blade 2 was replaced with the corresponding STE4 sequence, was less potent in activating locus ceruleus GIRK channels and in stimulating the PLC $\beta$ 2 activity. However, the present

study showed that a CD2 region mutant, G131V, which was less effective in activating GIRK channels (Fig. 3B), was able to activate PLC $\beta$ 2 as effectively as the wild-type G $\beta$ 1. This may mean that residues in the CD2 region other than Gly131 is involved with PLC $\beta$ 2 activation.

## Discussion

**Interaction among G $\alpha$ , G $\beta$ , and GIRK.** The signals initiated by G $\beta\gamma$  can be transmitted to downstream effectors (including GIRK channels) only if G $\alpha$  is dissociated from G $\beta\gamma$ . This feature suggested that the interaction domain between G $\beta$  and G $\alpha$  is shared with the interaction domain between G $\beta$  and effectors (Ford et al., 1998; Li et al., 1998). As to the interaction between G $\beta$  and GIRK1/GIRK4, the results by Ford et al. (1998) indicate that six G $\beta$ 1 residues located on the G $\beta$ /G $\alpha$  interface could be the interaction sites between G $\beta$  and GIRK (Fig. 6A,  $\circ$ ). Furthermore, Albsoul-Younes et al. (2001), using GIRK channel in brain neurons (presumably GIRK1/GIRK2), found that two more residues on G $\beta$ 1, Trp332, and Asp246, belong to this group (Fig. 6A,  $\square$ ).

G $\beta$ 5 is a particular type of G $\beta$  subunit. G $\beta$ 5 *inhibits* the GIRK channel, whereas all other G $\beta$ s activate it (Lei et al., 2000). Mirshahi et al. (2002) have recently determined the G $\beta$  residues that are responsible for this difference; these residues may be the interaction sites between G $\beta$  and GIRK. Their results indicate that Ser67 and Thr128 of G $\beta$  (Fig. 6A,  $\bullet$ ) may be the location of G $\beta$ /GIRK interaction. These sites are located outside the G $\beta$ /G $\alpha$  interaction domain.

Albsoul-Younes et al. (2001) used STE4 to search for the G $\beta$ /GIRK interaction sites. STE4, being the member of the G $\beta$  family that is most distantly related to mammalian G $\beta$ s, does not activate GIRK (Peng et al., 2000). Albsoul-Younes et al. (2001) constructed a set of chimera DNAs, in which the sequence at or near the outer  $\beta$  strand of each blade was replaced by the corresponding sequence of STE4. The mutant G $\beta$ 1 $\gamma$ 2 proteins were purified and were tested on native GIRK channels in locus ceruleus neurons. Substitution of STE4 outer strands of blades 1 and 2 for the wild type resulted in impairment of GIRK channel activation, suggesting that some residues on the outermost sheets of blades 1 and blade 2 are the G $\beta$ /GIRK interaction sites.

In the present study, we used genetically identified GIRK channels (GIRK1/GIRK2) instead of native GIRK channels in locus ceruleus neurons. By creating point mutations on the regions identified previously (Albsoul-Younes et al., 2001), we have localized the G $\beta$  residues that are responsible for the functional impairment of the chimera between STE4 and G $\beta$ 1. Our results indicate that three residues on G $\beta$ 1 (Thr86, Thr87, and Gly131; Fig. 6A,  $\blacksquare$ ) are putative interaction sites between G $\beta$ 1 and GIRK. It is noted that all three residues are located *outside* the G $\beta$ /G $\alpha$  contact points and they are all located at sites accessible from outside (Fig. 6B). Together with the work by Mirshahi et al. (2002), there are now five residues of this category (Fig. 6A, filled symbols), suggesting that the functional roles of these residues are not trivial. Interestingly, all five residues are located on the loops connecting the  $\beta$  strands; this arrangement is consistent with the notion that active sites of protein-protein interactions are often located on loops between  $\beta$ -strands.

In summary (Ford et al., 1998; Albsoul-Younes et al., 2001;

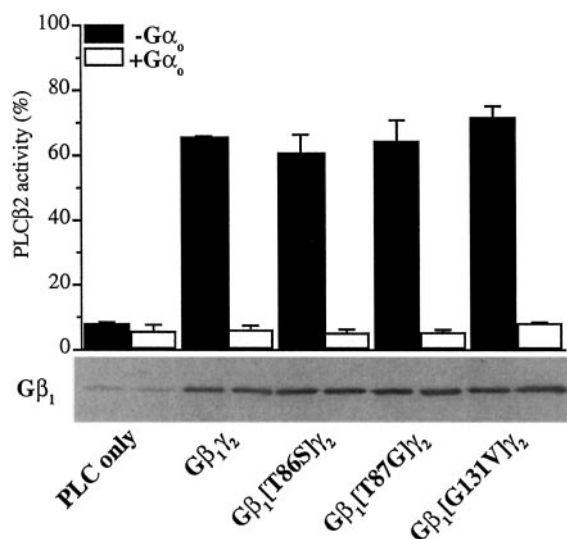


**Fig. 5.** Activation of PLC $\beta$ 2 by G $\beta$ 1 mutants. HEK293 cells in 24-well plates were transfected with 0.2  $\mu$ g of each kind of cDNA. In all cases, vector DNA was added to give a final DNA concentration of 0.8  $\mu$ g/well. The activity of PLC $\beta$ 2 was expressed as the ratio of the amount of inositol phosphates to the total amount of free inositol and inositol phosphates. The data shown are representatives of three experiments. The error bars indicate the S.E.M. of duplicate assays.  $\blacksquare$ , without G $\alpha_o$ ;  $\square$ , with G $\alpha_o$ . Bottom, immunoblots of triplicate samples in the same experiment.



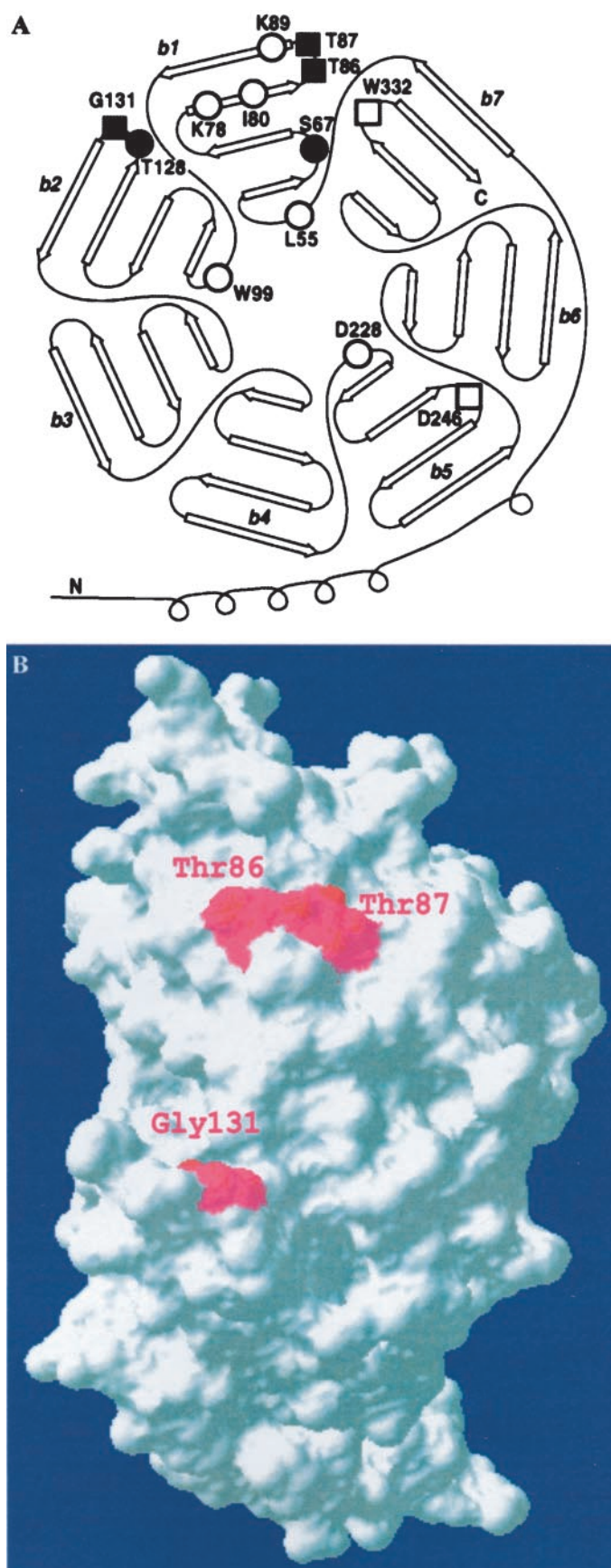


**Fig. 6.** Interaction sites on G $\beta$ 1 for GIRK channels. A, a diagram of G $\beta$ 1 $\gamma$ 2 based on the published structures by Wall et al. (1995) and Lambricht et al. (1996). The seven blades of the G $\beta$ 1 propeller were

Mirshahi et al., 2002; present study), there are three domains that are involved in the interaction among G $\beta$ , G $\alpha$ , and GIRK: 1) a G $\beta$ /GIRK interaction area outside the G $\beta$ /G $\alpha$  interaction site (Fig. 6A, filled symbols), 2) an area belonging both to the G $\beta$ /G $\alpha$  interaction sites and to the G $\beta$ /GIRK interaction sites (Fig. 6A, open symbols), and 3) an area belonging to the G $\beta$ /G $\alpha$  interaction region but outside the G $\beta$ /GIRK interaction sites (not shown). In other words, the G $\beta$ /G $\alpha$  interaction area and the G $\beta$ /GIRK interaction area are not identical, but the two areas intersect.

**Protein-Protein Interactions Involving G $\beta\gamma$ .** Various signaling pathways from many receptors converge on G proteins. Convergence is caused by the simple fact that the same G proteins couple to many different receptors. The signals then diverge from the G proteins to multiple effectors such as GIRK, calcium channels, PLC $\beta$ s, and adenylyl cyclases. The results from this study and others have revealed that these effectors (or any interacting proteins) associate with G $\beta\gamma$  through both the G $\alpha$ -interacting surface and part of the outer-surface of the blade structure. It has also become clear that each of these proteins is using a specific part of the outer surface of G $\beta$ . Certain mutations of the outer strands of blades 2, 6, and 7 impair PLC $\beta$ 2 activation but not the regulation of adenylyl cyclases (Panchenko et al., 1998; Albsoul-Younes et al., 2001). Mutations of certain residues on the outer surface of blades 1 and 2 affected GIRK activation but not PLC $\beta$ 2 or adenylyl cyclase type II activation (Albsoul-Younes et al., 2001; present study). Phosducin binds G $\beta$  not only on the G $\beta$ /G $\alpha$  interaction site but also on the outer strands of blades 1 and 7. However, phosducin does not bind to the three putative G $\beta$ /GIRK interaction sites described in this study (Thr86, Thr87, and Gly131; Fig. 6A) (Gaudet et al., 1996). It seems that G $\beta$  is using its blade structure for the regulation of different nonhomologous effector molecules. This could be one of the mechanisms for achieving divergence of signaling.

On the other hand, certain residues on G $\beta$  seem to play a more universal role for the protein-protein interaction. One of them is Trp332. Alanine mutation of the Trp332 residue in G $\beta$ 1 impaired the subunit's ability to activate GIRK1/GIRK2 (Fig. 1C) as well as the native GIRK channel in locus ceruleus (Albsoul-Younes et al., 2001). Recently, Nishida and MacKinnon (2002), based on their crystallographic study of N- and C-termini of GIRK and in analogy with the interaction sites between phosducin and G $\beta$  (Gaudet et al., 1996), proposed the idea that the  $\alpha$ -helix near the end of the GIRK C terminus may interact with G $\beta$  at Trp332. It is known that not only is Trp332 an interaction site between G $\beta$  and GIRK and between G $\beta$  and phosducin but also between G $\beta$  and G $\alpha$  (Lam-

labeled as b1 to b7, following the designation of Wall et al. (1995).  $\circ$ , eight G $\beta$ 1 residues belonging to both the G $\beta$ /G $\alpha$  interaction sites and the G $\beta$ /GIRK interaction sites (Leu55, Lys78, Ile80, Lys89, Trp99, and Asp228), identified by Ford et al. (1998).  $\square$ , Asp246 and Trp332 also belong to both the G $\beta$ /G $\alpha$  interaction sites and the G $\beta$ /GIRK interaction site, described by Albsoul-Younes et al. (2001). Filled symbols belong to the G $\beta$ /GIRK interaction sites outside G $\beta$ /G $\alpha$  interaction sites: Ser67 and Thr128 ( $\bullet$ ) were identified by Mirshahi et al. (2002), and Thr86, Thr87 and Gly131 ( $\blacksquare$ ) were identified in the present study. B, three-dimensional surface of G $\beta\gamma$  complex. The three G $\beta$ 1 residues (Thr86, Thr87, and Gly131; pink), which are putative interaction sites between G $\beta$ 1 and GIRK1/2, reside on the surface of the G $\beta$  subunit. The figure was generated with the program Deepview/Swiss-pdb Viewer (Glaxo SmithKline R and D; version 3.7) using published coordinates of G $\beta\gamma$  (Sondek et al., 1996).

bright et al., 1996). In addition, Trp332 interacts with several effectors such as PLC $\beta$ 2, PLC $\beta$ 3, and adenylyl cyclase 2 (Ford et al., 1998; Li et al., 1998). In this respect, Trp332 seems to be a universally key residue for the protein-protein interactions involving G $\beta$ .

One of the marked differences between G $\beta$ /G $\alpha$  association and G $\beta$ /phosducin association is that the former association does not entail conformational changes of G $\beta$  (Lambright et al., 1996), whereas the latter does (Gaudet et al., 1996; Loew et al., 1998). Because of certain similarities between the G $\beta$ /phosducin association and the G $\beta$ /GIRK association, the question arises of whether conformational changes of G $\beta$  occur accompanying the G $\beta$ /GIRK interaction. Crystallographic studies will answer this.

#### Acknowledgments

The cDNA of W332A was originally constructed in the laboratory of the late Dr. Eva Neer. Thanks are owed to Moritz Bünemann for suggestions on the culturing technique of HEK293 cells. We thank Tohru Yamada, Constance J. Jeffery, and Diana Arsenieva for help in generating the three-dimensional surface of G $\beta$  $\gamma$  complex and John M Collins for suggestions in the writing.

#### References

- Albsoul-Younes AM, Sternweis PM, Zhao P, Nakata H, Nakajima S, Nakajima Y, and Kozasa T (2001) Interaction sites of the G protein  $\beta$  subunit with brain G protein-coupled inward rectifier K $^{+}$  channel. *J Biol Chem* **276**:12712–12717.
- Andersson S, Davis DL, Dahlback H, Jornvall H, and Russell DW (1989) Cloning, structure and expression of the mitochondrial cytochrome P-450 sterol 26-hydroxylase, a bile acid biosynthetic enzyme. *J Biol Chem* **264**:8222–8229.
- Breitwieser GE and Szabo G (1985) Uncoupling of cardiac muscarinic and  $\beta$ -adrenergic receptors from ion channels by a guanine nucleotide analogue. *Nature (Lond)* **317**:538–540.
- Dascal N, Schreiber W, Lim NF, Wang W, Chavkin C, DiMaggio L, Labarca C, Kieffer BL, Gaveriaux-Ruff C, Trollinger D, et al. (1993) Atrial G protein-activated K $^{+}$  channel: expression cloning and molecular properties. *Proc Natl Acad Sci USA* **90**:10235–10239.
- Ford CE, Skiba NP, Bae H, Daaka Y, Reuveny E, Shekter LR, Rosal R, Weng G, Yang CS, Iyengar R, et al. (1998) Molecular basis for interactions of G protein  $\beta$  subunits with effectors. *Science (Wash DC)* **280**:1271–1274.
- Gaudet R, Bohm A, and Sigler PB (1996) Crystal structure at 2.4 angstroms resolution of the complex of transducin  $\beta\gamma$  and its regulator, phosducin. *Cell* **87**:577–588.
- Huang CL, Slesinger PA, Casey PJ, Jan YN, and Jan LY (1995) Evidence that direct binding of G $\beta\gamma$  to the GIRK1 G protein-gated inwardly rectifying K $^{+}$  channel is important for channel activation. *Neuron* **15**:1133–1143.
- Ito H, Tung RT, Sugimoto T, Kobayashi I, Takahashi K, Katada T, Ui M, and Kurachi Y (1992) On the mechanism of G protein  $\beta$  gamma subunit activation of the muscarinic K $^{+}$  channel in guinea pig atrial cell membrane. Comparison with the ATP-sensitive K $^{+}$  channel. *J Gen Physiol* **99**:961–983.
- Kawano T, Chen L, Watanabe SY, Yamauchi J, Kaziro Y, Nakajima Y, Nakajima S, and Itoh H (1999) Importance of the G protein gamma subunit in activating G protein-coupled inward rectifier K $^{+}$  channels. *FEBS Lett* **463**:355–359.
- Krapivinsky G, Krapivinsky L, Wickman K, and Clapham DE (1995) G  $\beta$  binds directly to the G protein-gated K $^{+}$  channel, I $K_{ACH}$ . *J Biol Chem* **270**:29059–29062.
- Kubo Y, Reuveny E, Slesinger PA, Jan YN, and Jan LY (1993) Primary structure and functional expression of a rat G-protein coupled muscarinic potassium channel. *Nature (Lond)* **364**:802–806.
- Kurachi Y, Nakajima T, and Sugimoto T (1986) On the mechanism of activation of muscarinic K $^{+}$  channels by adenosine in isolated atrial cells: involvement of GTP-binding proteins. *Pfluegers Arch Eur J Physiol* **407**:264–274.
- Lambright DG, Sondek J, Bohm A, Skiba NP, Hamm HE, and Sigler PB (1996) The 2.0 Å crystal structure of a heterotrimeric G protein. *Nature (Lond)* **379**:311–319.
- Lei Q, Jones MB, Talley EM, Schrier AD, McIntire WE, Garrison JC, and Bayliss DA (2000) Activation and inhibition of G protein-coupled inwardly rectifying potassium (Kir3) channels by G protein  $\beta\gamma$  subunits. *Proc Natl Acad Sci USA* **97**:9771–9776.
- Li Y, Sternweis PM, Charnecki S, Smith TF, Gilman AG, Neer EJ, and Kozasa T (1998) Sites for G $\alpha$  binding on the G protein  $\beta$  subunit overlap with sites for regulation of phospholipase C $\beta$  and adenylyl cyclase. *J Biol Chem* **273**:16265–16272.
- Loew A, Ho Y-K, Blundell T, and Bax B (1998) Phosducin induces a structural change in transducin  $\beta\gamma$ . *Structure* **6**:1007–1019.
- Logothetis DE, Kurachi Y, Galper J, Neer EJ, and Clapham DE (1987) The  $\beta\gamma$  subunits of GTP-binding proteins activate the muscarinic K $^{+}$  channel in heart. *Nature (Lond)* **325**:321–326.
- Mirshahi T, Robillard L, Zhang H, Hebert TE, and Logothetis DE (2002) G $\beta$  residues that do not interact with G $\alpha$  underlie agonist-independent activity of K $^{+}$  channels. *J Biol Chem* **277**:7348–7355.
- Nishida M and MacKinnon R (2002) Structural basis of inward rectification. Cytoplasmic pore of the G protein-gated inward rectifier Kir3.1 at 1.8 Å resolution. *Cell* **111**:957–965.
- Panchenko MP, Saxena K, Li Y, Charnecki S, Sternweis PM, Smith TF, Gilman AG, Kozasa T, and Neer EJ (1998) Sites important for PLC $\beta$ 2 activation by the G protein  $\beta\gamma$  subunit map to the sides of the  $\beta$  propeller structure. *J Biol Chem* **273**:28298–28304.
- Peng L, Zhang H, Hirsch J, and Logothetis DE (2000). The yeast  $\beta\gamma$  subunits of G proteins inhibit GIRK4 channels. *Biophysical J* **78**: 465A.
- Pfaffinger PJ, Martin JM, Hunter DD, Nathanson NM, and Hille B (1985) GTP-binding proteins couple cardiac muscarinic receptors to a K channel. *Nature (Lond)* **317**:536–538.
- Reuveny E, Slesinger PA, Inglese J, Morales JM, Iniguez-Lluhi JA, Lefkowitz RJ, Bourne HR, Jan YN, and Jan LY (1994) Activation of the cloned muscarinic potassium channel by G protein  $\beta\gamma$  subunits. *Nature (Lond)* **370**:143–146.
- Sakmann B, Noma A, and Trautwein W (1983) Acetylcholine activation of single muscarinic K $^{+}$  channels in isolated pacemaker cells of the mammalian heart. *Nature (Lond)* **303**:250–253.
- Sondek J, Bohm A, Lambright DG, Hamm HE, and Sigler PB (1996) Crystal structure of a G-protein  $\beta\gamma$  dimer at 2.1 Å resolution. *Nature (Lond)* **379**:369–374.
- Stanfield PR, Nakajima S, and Nakajima Y (2002) Constitutively active and G-protein coupled inward rectifier K $^{+}$  channels: Kir2.0 and Kir3.0. *Rev Physiol Biochem Pharmacol* **145**:47–179.
- Wall MA, Coleman DE, Lee E, Iniguez-Lluhi JA, Posner BA, Gilman AG, and Sprang SR (1995) The structure of the G protein heterotrimer G $\alpha_{i1}\beta_{1\gamma 2}$ . *Cell* **83**:1047–1058.
- Wickman K and Clapham DE (1995) Ion channel regulation by G proteins. *Physiol Rev* **75**:865–885.
- Zhao Q, Kawano T, Kozasa T, Nakajima Y, and Nakajima S (2002) Interaction sites of G protein  $\beta$  gamma subunit for Kir3 channels. *Soc Neurosci Abstr* **28**:17.5

**Address correspondence to:** Tohru Kozasa, Department of Pharmacology, College of Medicine, University of Illinois at Chicago, 835 S. Wolcott Ave., Chicago, IL 60612. E-mail: tkozasa@uic.edu